Nuclear Data for Science and Technology (1988 MITO), 717- 720, Copyright © 1988 JAERI.

ON THE TWO GAS COMPONENT EXCITON MODEL

G.Reffo, M.Herman, C.Costa

Ente Nazionale Energie Alternative, Divisione di Calcolo
40138 BOLOGNA, ITALY

Abstract: The two-component exciton model is reformulated to facilitate a solution of the master equation and to express transition rates via quasiparticle state densities calculated in the frame of the shell model. On this basis, flux flow between different substages of the composite nucleus is discussed. This analysis shows strong discrepancies in the strength of various transitions. In particular, particle-hole creation by a hole is found to be rather negligible.

(exciton model, state density, composite system equilibration)

Introduction

In description of the preequilibrium decay one-component models are used nearly exclusively. A consistent derivation of the effective one-component exciton model from the two component formulation was given by Gupta /1/. It was shown that, in a one-component model, transitions inconsistent with the assumption of the two-body nature of the equilibration process are included, and that this can be compensated by modification of the averaged matrix element $|M|^2$ without affecting the cross section and spectra predictions. However, it is only valid if the state densities for equivalent proton and neutron configurations are the same. Our recent shell-model calculations /2,3/ indicate that the assumption of an equal state density for neutron and proton configurations, that underlies the model by Gupta /1/, usually does not hold. To account for different neutron and proton state densities an explicit two-component formulation of the exciton model is inevitable.

Use of the one-component model also leads to an unavoidable inconsistency in the state densities for the preequilibrium and the equilibrium part. This deficiency is overcome naturally using the two-component formula for the densities of states with a fixed number of excitons, but this again implies use of the two-component model.

Two-component exciton model

The model, we report herein, is a natural extension of the exciton model to a system of two distinguishable components, as proposed by Dobes and Betak /4/. States are clssified according to the reaction stage number N and to the number of proton holes h_π. It is important to note that, while for N only the condition N>0 holds, the values of h_π are limited to $0 \leqslant h_\pi < N$. Using this representation the equilibration of the composite nucleus can be depicted on a two dimensional plot, as shown in Fig.1 for the case of a neutron projectile. The master equation describing equilibration of the two-component system is written

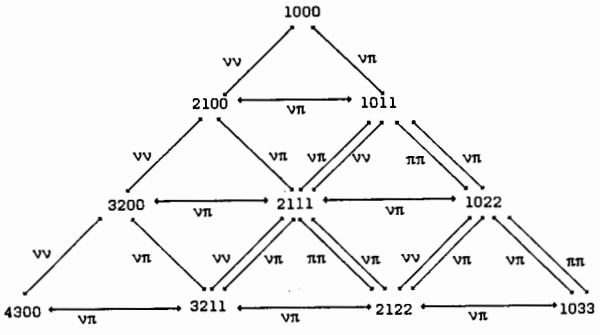

Fig.1. Schematic diagram of the equilibration of the composite nucleus formed in the neutron induced reaction. Different substages are denoted with p_ν, h_ν, p_π, and h_π. The arrows are labeled with the type of the interacting nucleons.

$$
\begin{aligned}
\frac{dP(N,h_\pi,t)}{dt} = {} & \left(\lambda^{++}_{\nu\pi}(E,N-1,h_\pi-1) + \lambda^{++}_{\pi\pi}(E,N-1,h_\pi-1)\right) P(N-1,h_\pi-1,t) \\
& + \left(\lambda^{+0}_{\pi\nu}(E,N-1,h_\pi) + \lambda^{+0}_{\nu\nu}(E,N-1,h_\pi)\right) P(N-1,h_\pi,t) \\
& + \left(\lambda^{-0}_{\nu\nu}(E,N+1,h_\pi) + \lambda^{-0}_{\pi\nu}(E,N+1,h_\pi)\right) P(N+1,h_\pi,t) \\
& + \left(\lambda^{--}_{\pi\pi}(E,N+1,h_\pi+1) + \lambda^{--}_{\pi\nu}(E,N+1,h_\pi+1)\right) P(N+1,h_\pi+1,t) \\
& + \lambda^{0+}_{\nu\pi}(E,N,h_\pi-1)\ P(N,h_\pi-1,t) \\
& + \lambda^{0-}_{\pi\nu}(E,N,h_\pi+1)\ P(N,h_\pi+1,t) \\
& - \Big(\lambda^{+0}_{\nu\nu}(E,N,h_\pi) + \lambda^{+0}_{\pi\nu}(E,N,h_\pi) + \lambda^{++}_{\nu\pi}(E,N,h_\pi) + \lambda^{++}_{\pi\pi}(E,N,h_\pi) \\
& + \lambda^{--}_{\pi\nu}(E,N,h_\pi) + \lambda^{--}_{\pi\pi}(E,N,h_\pi) + \lambda^{-0}_{\nu\pi}(E,N,h_\pi) + \lambda^{-0}_{\nu\nu}(E,N,h_\pi) \\
& + \lambda^{0-}_{\pi\nu}(E,N,h_\pi) + \lambda^{0+}_{\nu\pi}(E,N,h_\pi) + W(E,N,h_\pi)\Big) P(N,h_\pi,t)
\end{aligned}
\qquad (1)
$$

Here, P is a population of N, h_π substage at time t, and λ are internal transition rates. Two superscripts indicate a change in N and h_π, while the subscripts stand for the types of both interacting nucleons. The emission rates $W(E,N,h_\pi)$ are written in analogy to the one-component exciton model, having one-gas state densities replaced by the two-gas quantities.

To facilitate the solution of the master equation we transform the two-dimensional population matrix into a vector. We note, that because of $h_\pi < N$, the population matrix in Eq.1 is in fact triangular. Accordingly, we can ascribe a running index 'j' to each substage starting

from the top of Fig.1 and enumerating along subsequent rows from the left to the right. The new index 'j' is related to N and h_π by a simple relation

$$j = N(N-1)/2 + h_\pi + 1, \qquad (2)$$

and is sufficient to specify a substage completely. N and h_π may be obtained for each 'j' through the expressions

$$N = INT(0.5 + \sqrt{2j - 1.75}) \qquad (3)$$

and

$$h_\pi = j - N(N-1)/2 \qquad (4)$$

where INT stands for the Entier function. This way, the Eq.1 has been transformed into the standard system of linear differential equations. To specify it, we have to write the matrix in Eq.1 in terms of 'j'. Let us note, that in the (N,h_π) representation the following 'selection rules' for the internal transitions hold

$$\Delta N=-1;\ \Delta h_\pi=-1,\ 0$$
$$\Delta N=\ 0;\ \Delta h_\pi=\ 1,-1$$
$$\Delta N=\ 1;\ \Delta h_\pi=\ 0,\ 1$$

with boundary conditions $N>0$ and $0 \leq h_\pi < N$. Transforming these selection rules to the j representation, it is easy to show that a given substage j is coupled to the following i substages

i=j-N+1 and i=j-N through $\Delta N=-1$ transitions with boundary condition $(N-2)(N-1)/2 < i \leq N(N-1)/2$

i=j+1 and i=j-1 through $\Delta N=0$ transitions with the boundary condition $N(N-1)/2 < i \leq N(N+1)/2$

i=j+N and i=j+N+1 through the $\Delta N=1$ transitions with no boundary condition.

In Fig.2 we show that the two-component master equation indexed with j nicely links to the one-component version. To elucidate this feature, the thick horizontal and vertical lines are drawn to separate the reaction stages. Clearly, master equation matrix remains tri-diagonal in the N representation, which corresponds to the one-component model.

Internal transition rates.

Assuming two-body interaction, there are 18 diagrams that contribute to internal transitions (Fig.3). Following Fermi's Golden Rule, a transition rate λ is proportional to average squared matrix element and to the density of final accessible states.

The density of accessible states is calculated as follows. First, the system is split into the interacting part, which contains the excitons taking part in the interaction, and the passive part that behaves like a spectator. The probability of finding the required interacting part with energy ε is given by the ratio of the state density of the passive part at energy $E-\varepsilon$ to the density of states for the whole system at energy E. The total number of interacting configurations is obtained as a product of the above probability and the density of states for the interacting part. To obtain the density of accessible states, we multiply the above with the density of the interacting part in the final state and integrate over ε from 0 to E. This simple procedure requires performing one numerical integration if the state densities are given in a tabulated form, whereas analytical expressions are straightforward if state densities are given in terms of the energy polynomials. For example, the density of accessible states associated with the third diagram reads

N		1	2		3			4			
	j	1	2	3	4	5	6	7	8	9	10
1	1	L	λ^{-0}	λ^{--}							
2	2	λ^{+0}	L	λ^{0-}	λ^{-0}	λ^{--}					
	3	λ^{++}	λ^{0+}	L		λ^{-0}	λ^{--}				
3	4		λ^{+0}		L	λ^{0-}		λ^{-0}	λ^{--}		
	5		λ^{++}	λ^{+0}	λ^{0+}	L	λ^{0-}		λ^{-0}	λ^{--}	
	6			λ^{++}		λ^{0+}	L			λ^{-0}	λ^{--}
4	7				λ^{+0}			L	λ^{0-}		
	8				λ^{++}	λ^{+0}		λ^{0+}	L	λ^{0-}	
	9					λ^{++}	λ^{+0}		λ^{0+}	L	λ^{0-}
	10						λ^{++}			λ^{0+}	L

Fig.2. Schematic representation of the j-indexed master equation. Thick lines separate different stages of the equilibration process. Off-diagonal elements represent gain of the flux from other substages, while diagonal elements L are responsible for the loss of the flux due to the coupling to other substages and to the open channels.

$$^{3}\omega^{++}_{\nu\pi}(E) = \int_0^E \frac{\omega(E-\varepsilon,p_\nu-1,h_\nu,p_\pi,h_\pi)}{\omega(E,p_\nu,h_\nu,p_\pi,h_\pi)}\,\omega(\varepsilon,1,0,0,0)\cdot \qquad (5)$$
$$\omega(\varepsilon,1,0,1,1)\,d\varepsilon$$

Similar expressions for the remaining 17 diagrams are easily obtainable applying the above procedure.

The transition rates are obtained by applying the Golden Rule and summing the appropriate diagrams of Fig.3.

The analytical expressions for the accessible state densities are obtained using the two-component formula for state densities /5/

$$\omega(E,p_\nu,h_\nu,p_\pi,h_\pi) = \frac{g_\nu^{p_\nu}\,\tilde{g}_\nu^{h_\nu}\,g_\pi^{p_\pi}\,\tilde{g}_\pi^{h_\pi}\,(E-S)^{n-1}}{p_\nu!\,h_\nu!\,p_\pi!\,h_\pi!\,(n-1)!}\,\Theta(E-T) \qquad (6)$$

Note that single particle state densities for particles g and for holes $\tilde{g}$ are differentiated. Energy shift S contains the Pauli correction and, eventually, pairing shift. In Eq.6 we include also Heaviside function $\theta(E-T)$, which excludes states below the threshold T for a given exciton configuration, thus accounting for the most important effect of the shell structure. Using Eq.6 expressions analogous to Eq.5 can be integrated analytically.

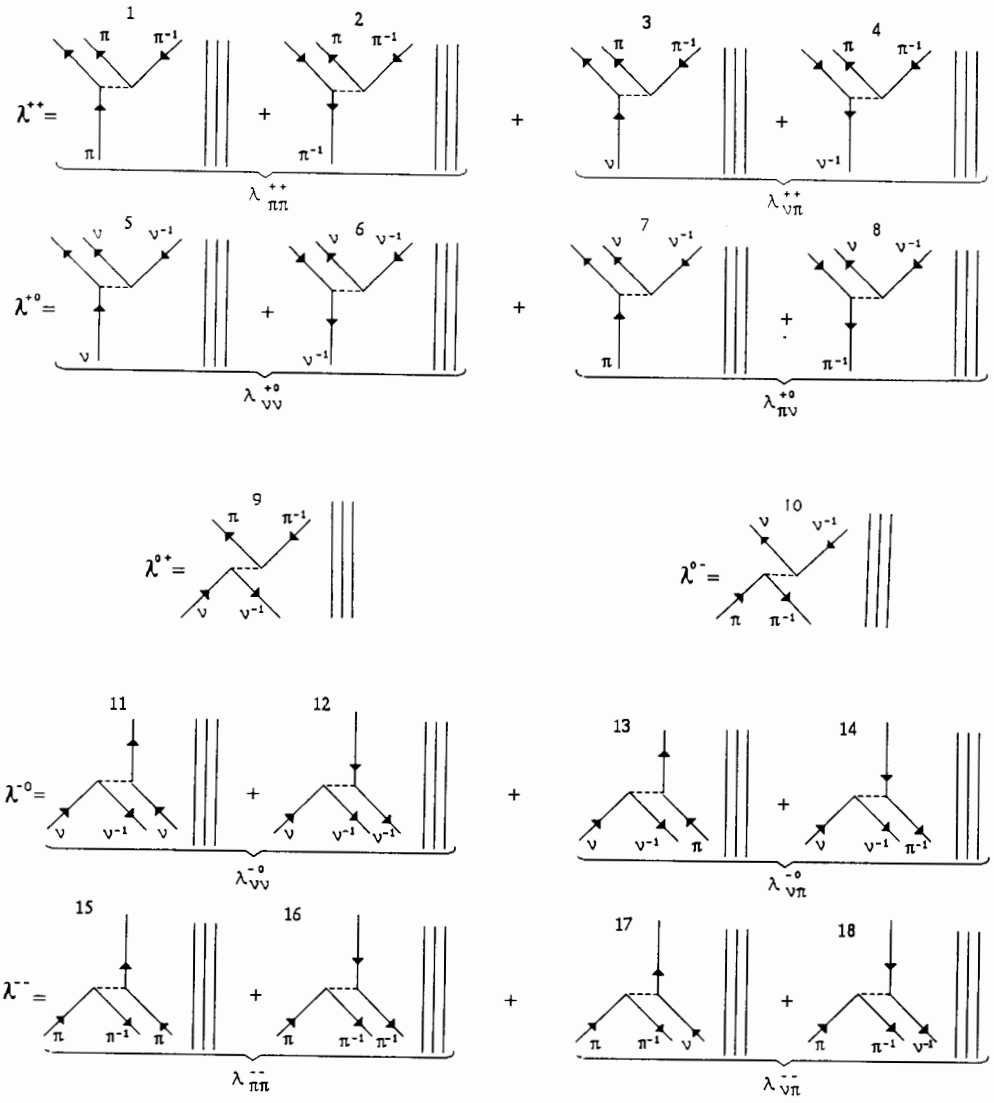

Fig.3. Diagrams illustrating internuclear transitions in the two-component exciton model. Interacting particles (holes) are represented by upward (downward) arrows, and their nucleon type is indicated. Vertical lines stand for the passive excitons. The diagrams are enumerated to facilitate reference.

Equilibration of a composite nucleus

Flow of the flux through particular substages of the composite system may be qualitatively discussed on the basis of the transition rates, without solving master equation. Assuming all matrix elements equal, discussion can be carried out in terms of the accessible state densities.

Accessible state densities were obtained, performing numerical integration of Eq.5, in which microscopically calculated state densities were used. Microscopic calculations were performed according to the method described in Refs.2 and 3 in the space of the shell-model orbitals as determined by Nix and Möller /6/. No explicit interactions between particles was assumed. To simulate natural level width and configuration mixing, a Gaussian strength distribution was ascribed to each nuclear state.

To demonstrate clearly the effects of the shell structure, we choose 90Zr, which is a magic nucleus in respect to neutrons while protons fill roughly half of the shell. Let us concentrate on the (2100) and (1011) configurations. In Fig.4 several representative accessible state densities, associated with the appropriate decay processes (see Fig.3) of both configurations are shown.

In the decay of (2100) configuration, creation of the proton particle-hole pair by a neutron particle (diagram 3) is a leading process. Creation of the neutron particle-hole pair (diagram 5) becomes only important above 20 MeV of excitation energy and is by factor of 2 less probable. We note, that analogous transition caused by the neutron hole (diagram 6) is an order of magnitude weaker. The intersubstage transitions are realized via diagram 9. Accessible state density for this process is found to be approximately 10 times lower than for the leading (exciton creating) diagrams. For the backward

transitions (diagram 11) the same ratio exceeds 100.

In the case of the (1011) configuration only most important transitions are shown in Fig.4. Below 12 MeV of excitation energy the configuration decays nearly exclusively via the proton pair creation induced by the neutron particle (diagram 3). Above this energy, also other decay modes become possible. Accessible state densities for these transitions differ from each other by up to an order of magnitude.

In both cases strongest effect of the shell structure is observed at low excitation energies. Accessible state densities reveal thresholds, that are scattered over a broad energy range (between 4 and 14 MeV in the case of 1011 configuration decay in 90Zr). In this low energy region, one may thus expect strongly nonuniform flow of the flux through different substages. In general, due to the Pauli principle accessible state densities for the unlike transitions are higher than those for the like ones. Therefore, one expects that in any way formed composite system will proceed to its equilibrium containing equal number of proton and neutron degrees of freedom, and that the main part of the flux will pass through the substages laying in the middle of the graph shown in Fig.1.

Let us now discuss the flow of the flux through various substages during the equilibration of the 90Zr excited to 18.5 MeV as a result of the neutron absorption. We will take into account only forward transitions, since neglect of the backward and N=0 transitions is fully justified for the first stages of the equilibration chain. The initial configuration (1000) may decay to (2100) and to (1011) substages. Assuming the decay proportional to the state densities in the appropriate substage we find that 33% of the flux will go to the (2100) substage, while the population of the (1011) substage will be twice as high (67%). The (2100) substage will decay predominantly to the (2111) substage (83%), and only with 17% to the (3200). The second N=2 substage (1011) will populate (2111) and (1022) nearly equally (53% and 47% respectively). Thus we expect following partition of the flux between 3 substages with N=3: 6% for (3200), 63% for (2111),and 31% for (1022). This confirms our predictions of nonuniform population probability for the different substages of a given reaction stage. In this particular case, we may expect enhanced proton emission compared to the predictions of the one-component model.

Conclusions

The reformulation of the two-component exciton model presented in this paper consists in the introduction of the microscopically calculated densities of quasiparticle states, and transformation of the master equation to the form in which it can be easily solved using standard numerical methods.

Analysing transition rates for the decay of the initial stages of the composite nucleus we have shown that, due to the shell structure, a nonuniform flow of the flux through different substages is expected.

It has been found that the leading decay mode is the creation of the particle-hole pair of a given nucleon type by a particle of the opposite nucleon type (unlike-type interaction). This implies that a system, during its equilibration, will tend to populate mostly substages with not too different number of neutron- and proton-type excitons. In addition, it turned out that transitions induced by the holes are strongly suppressed, due to the low density of the single particle states below the Fermi energy.

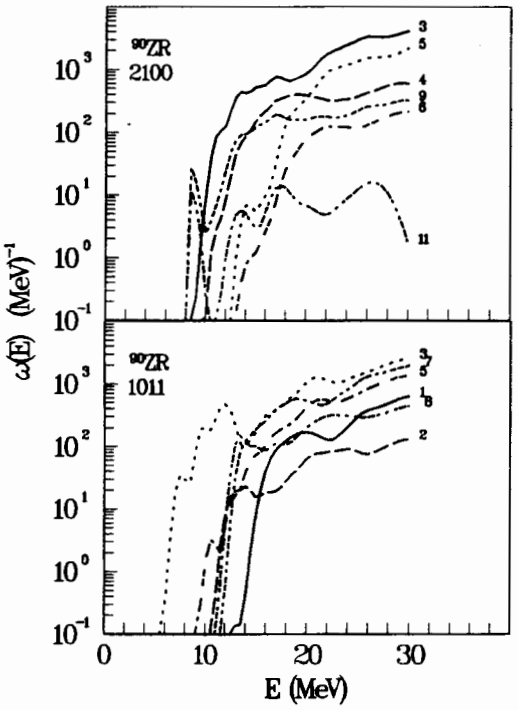

Fig.4. Accessible state densities for the decay of (2100) and (1011) substages in 90Zr as a function of excitation energy. Curves are denoted by numbers, which relate them to the appropriate diagrams of Fig.3.

List of references

1. S.K.Gupta, Z. Phys. A303,329(1981).
2. M.Herman and G.Reffo, Phys. Rev. C36,1546(1987).
3. M.Herman, G.Reffo, and R.A.Rego, Phys. Rev. C37,797(1988).
4. J.Dobes, and E.Betak, Z.Phys.A310,329(1983).
5. F.C.Williams Jr., Phys. Lett. 31B,184(1970).
6. J.R.Nix and P.Möller, private communication (1986).